JOURNAL OF Materials CHEMISTRY

Electroluminescent bipolar compounds containing quinoxaline or pyridopyrazine and triarylamine segments

K. R. Justin Thomas,[a] Jiann T. Lin,*[a,b] Yu-Tai Tao*[a] and C. H. Chuen[a]

[a] *Institute of Chemistry, Academia Sinica, 115 Nankang, Taipei, Taiwan.*
E-mail: jtlin@chem.sinica.edu.tw
[b] *Department of Chemistry, National Central University, 320 Chungli, Taiwan*

Received 25th June 2002, Accepted 3rd October 2002

Dipolar compounds containing both quinoxaline/pyridopyrazine acceptors and arylamine/carbazole donors have been prepared by palladium catalyzed C–C coupling (Stille) reactions in good yields and have been characterized by spectroscopic, electrochemical and thermal methods. The charge transfer character of these molecules can be changed by modification of the acceptor or donor ends. They are green emitting with moderate quantum yields in toluene solutions. However, in dichloromethane the emission maximum is red shifted and the quantum yield diminishes appreciably. High glass transition temperatures were realized for these compounds (143–162 °C). The quinoxaline derivatives effectively function as a hole-transporting and emitting layer in yellow/orange emitting double layer electroluminescent devices. We also demonstrate the possibility of using these materials in single layer devices.

Introduction

Donor–acceptor materials find much use in optoelectronic devices owing to their promising non-linear optical,[1] two-photon absorption[2] and red-shifted emission[3] properties. Organic light emitting diodes[4] (OLEDs) require amorphous films that are capable of carrying both holes and electrons. Dipolar compounds are ideal for this purpose. In recent years a wide array of dipolar compounds have been synthesized for electroluminescent applications. Prominent among them are oxadiazole/amine,[5,6] pyridine/quinolineamine,[7] thiophene or pyrrole/benzothiadiazole[8] and carbazole/cyanovinylene[9] combinations. Within this series oxadiazole–amine dyads received immense attention in recent years owing to their wide potential in non-liner optics and two-photon absorption.[10] Electron transfer between donor and acceptor in these molecules provides a method of efficient charge generation, which may benefit OLEDs.[11]

We have been interested in molecules that incorporate multiple functions for applications in OLEDs. Earlier we reported star shaped molecules and carbazole based pyrene amines and demonstrated their promising hole-transporting and emitting properties. In a continuation of our efforts[12–17] on the preparation of materials with both light-emitting and charge transporting properties for OLEDs, we report herein the synthesis of quinoxaline- and pyridopyrazine-based conjugated materials end-capped with donor fragments (carbazole or diphenylamine). A thiophene moiety is incorporated in the structure as it facilitates the synthesis of the target molecules. In addition, it is also expected that thiophene conjugation will lead to red-shifted emission. We have evaluated the function of these materials in double layer OLEDs by employing them as a hole-transporting and emitting layer. A quinoxaline segment has been used as a building block in hole-blocking or electron-transporting polymers and small molecules.[18,19] However, only recently have triarylamine–quinoxaline dyads and related derivatives been systematically explored as electroluminescent materials.[20,21]

Results and discussion

Synthesis and optical properties

The dipolar compounds were conveniently prepared by palladium catalyzed cross coupling reactions (Scheme 1) of the dibromides (**1** and **2**) with the corresponding stannylene derivatives in dimethyl formamide with good yields. The stannylene derivatives required for this study were available from an earlier work.[16] The dipolar materials are yellow or orange in color and soluble in most solvents excluding hydrocarbon solvents such as hexanes. In their absorption spectra they display a prominent band at *ca.* 390–410 nm (Table 1 and Fig. 1). It seems there is no notable solvent effect on this band and it is assigned as a π–π* transition. In compounds **5–8** (Chart 1), an additional high-energy transition with weaker

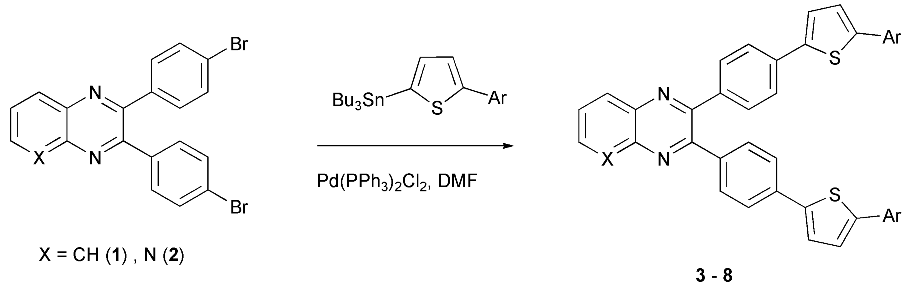

Scheme 1 Synthesis of compounds **3–8**.

DOI: 10.1039/b206126k

Table 1 Photophysical data for the donor–acceptor compounds

	In dichloromethane		In toluene		
Compound	λ_{abs}/nm ($\varepsilon_{max}/10^{-3}$ M^{-1} cm^{-1})	λ_{em}/nm (Φ_f (%))	λ_{abs}/nm ($\varepsilon_{max}/10^{-3}$ M^{-1} cm^{-1})	λ_{em}/nm (Φ_f (%))	T_g (T_d)/°C
3	390 (56.24) 309 (40.43)	572 (6)	401 (40.23)	497 (24)	146 (589)
4	393 (53.04)	624 (< 1%)	403 (36.36)	512 (17)	162 (574)
5	400 (85.44), 307 (52.84)	603 (~ 1)	402 (45.2), 307 (28.7)	502 (15)	134 (463)
6	402 (93.6), 306 (62.6)	—	408 (72.1), 305 (50.4)	537 (13)	148 (459)
7	403 (113.6), 315 (46.3)	612 (< 1)	404 (141.4), 313 (59.7)	496 (16)	150 (400)
8	409 (104.9), 313 (50.40)	—	405 (114.3), 313 (56.38)	524 (14)	154 (420)

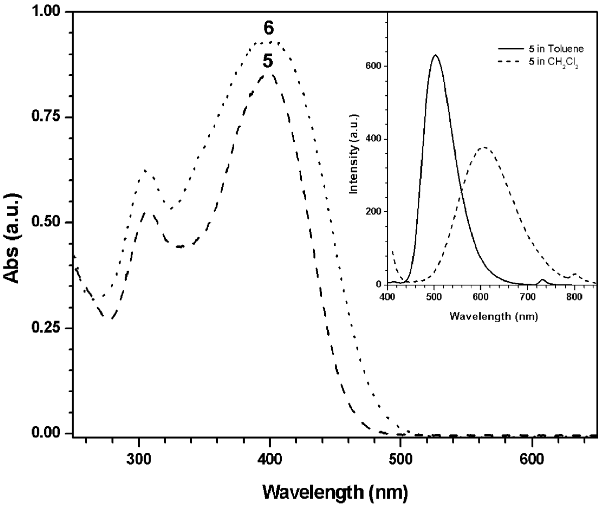

Fig. 1 Absorption spectra of compounds **5** and **6** in dichloromethane; and inset, emission spectra of compound **5** in toluene and dichloromethane.

transition probability is also realized. This is attributed to the *n*–π* transition arising from the terminal diphenylamine moieties.[15] No discrete charge transfer bands are found in these compounds and we assume that they are buried in the π–π* transition. All the compounds emit with moderate intensity in less polar solvents such as toluene in the green region. However on increasing the solvent polarity the emission intensity diminishes significantly with a concomitant red shift in the emission wavelength. This effect is more pronounced as the electron withdrawing strength or electron-donating strength increases. This indicates that relaxation to a more planar structure and/or dipolar interactions contribute to the non-radiative decay in these molecules.[6b,22] This influences the performance of the electroluminescent devices fabricated using these materials (*vide supra*).

Thermal properties

The glass forming capability and thermal stability of these dipolar materials were investigated by differential scanning calorimetry (DSC) and thermogravimetric analysis (TGA), respectively. The pertinent data are compiled in Table 1. All the compounds form glasses easily on heating and no crystallization was noticed even if the material was heated above the glass transition temperature (T_g). Similarly no melting exotherm was identified for these materials. The profound stability of the glassy state is remarkable and is uncommon for the diphenylamine-derivatized compounds.[4e] It should be noted that the glassy state is facilitated in a molecule if it incorporates non-planar structural elements and/or asymmetrically substituted triarylamines.[23,24] The T_g of these materials is significantly higher than the two classical hole-transporting materials TPD and α-NPD. The pyridopyrazine derivatives (**4**, **6** and **8**) possess slightly higher T_g when compared to their quinoxaline counterparts (**3**, **5** and **7**). The decomposition temperature of these materials is also promising. Among the compounds, the carbazole derivatives **3** and **4** inherit enhanced thermal stability. The role of carbazole in increasing the thermal stability of electroluminescent materials is well known in the literature.[12,14]

Electrochemical properties

The bipolar transport capability of a material can be identified from its propensity to stabilize both cation and anions. Electrochemical studies can be used as a rough estimation of the bipolar radical format character. We have studied these molecules by cyclic voltammetric measurements in dichloromethane and the redox potentials are reported in Table 2. All the molecules undergo a single-step two-electron reversible oxidation attributable to the carbazole or diphenylamine core and a one-electron quasi-reversible reduction arising from the quinoxaline or pyridopyrazine segment. The typical cyclic voltammetric behavior is shown in Fig. 2 for compound **8**. The redox potentials exhibit trends arising from the strength of the donor and acceptor segments. An additional two-electron oxidation wave observable at high positive potentials for compounds **5–8** probably stems from the thiophene segment. For compounds **3** and **4** this reversible oxidation is not visible, however, a new multi-electron irreversible oxidation peak is present at *ca.* 1.2 V. This wave may be due to the formation of dication radicals and thiophene oxidation.

Electroluminescent characteristics

The electrochemical potentials were used to obtain the orbital (HOMO and LUMO) energies in comparison with ferrocene, which has HOMO at 4.8 eV. The HOMO and LUMO energies of these molecules (Table 2) are located near the work function of ITO and the LUMO (2.70 eV)[14] of electron-transporting 1,3,5-tris(*N*-phenylbenzimidazol-2-yl)benzene (TPBI), respectively. Therefore, we speculate that these molecules can effectively function as bipolar transport layers in OLEDs. To ascertain the functional capability of these materials, initially we fabricated four devices using compound **3** with different device structures as follows: (i) ITO/**3** (800 nm)/Mg : Ag; (ii) ITO/NPD (400 nm)/**3** (400 nm)/Mg : Ag; (iii) ITO/**3** (400 nm)/TPBI (400 nm)/Mg : Ag; and (iv) ITO/**3** (400 nm)/Alq$_3$ (400 nm)/Mg : Ag, where Alq$_3$ is tris(8-hydroxyquinoline aluminium).

These configurations allow us to evaluate the role of these compounds in electroluminescent devices. Bright greenish yellow emission was realized for all the devices. The emission maxima resemble that of the pure vapor deposited film. Among the four devices, (iv) displays the best performance statistics (Table 3 and Fig. 3). This suggests that, despite the presence of low-lying LUMO, these molecules need improvement for electron transportation. Thus an efficient electron transporter, Alq$_3$, leads to an optimized device. Two types of devices of the configuration ITO/**X**/ETL/Mg : Ag (**X** = **4**, **5**, **6**, and **7**; ETL (electron transporting layer) = Alq$_3$ or TPBI) were fabricated

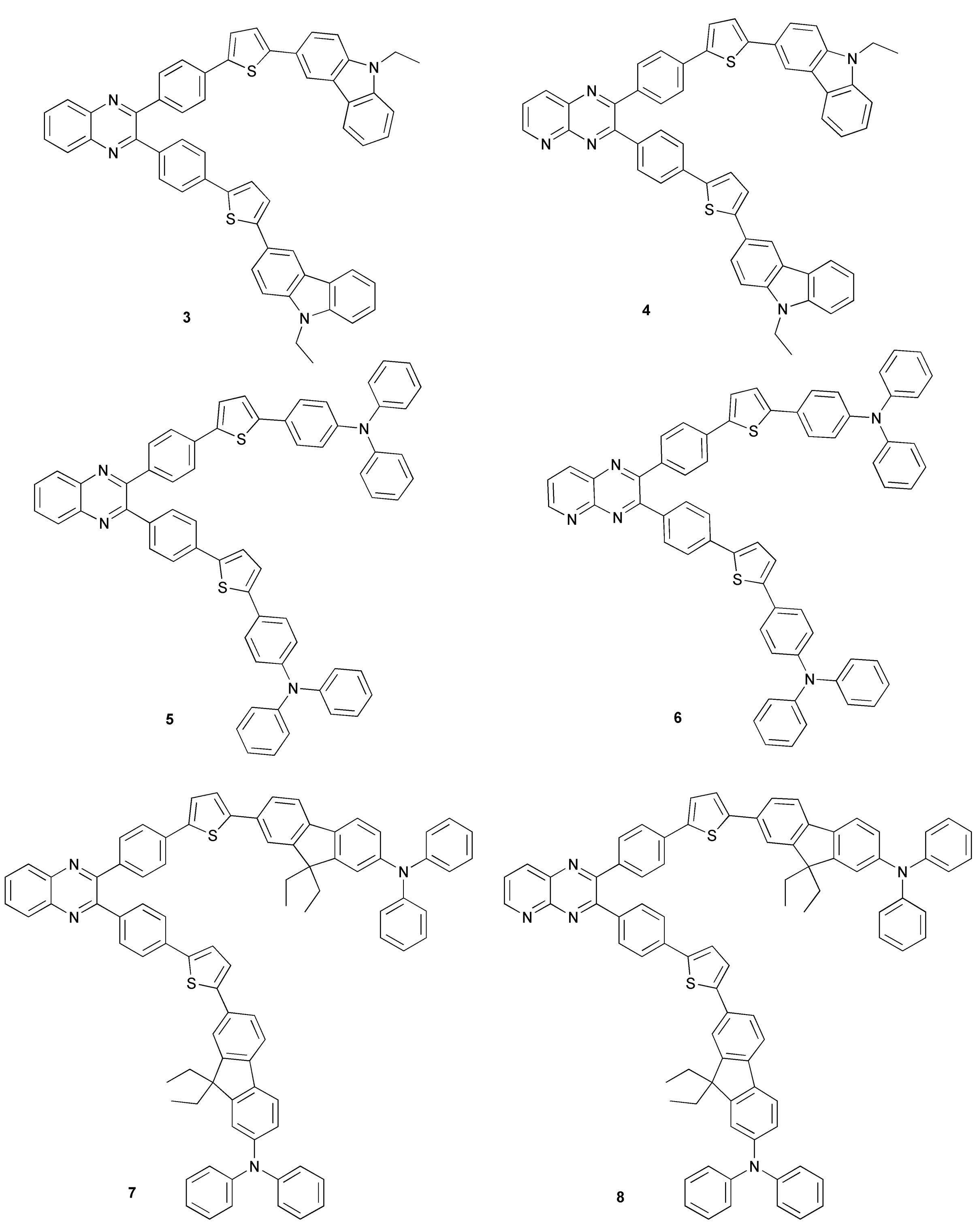
3

4

5

6

7

8

Chart 1

for the other molecules (**4**–**7**). Compounds **5** and **7** also exhibit good device characteristics when Alq$_3$ is used as the electron transporting material (Table 4 and Figs. 4 and 5). The observed electroluminescence (EL) and film photoluminecence (PL) spectra are displayed in Fig. 6 for compound **7**. From the figure it is evident that excitons are confined to the hole transporting layer (HTL) layer for both TPBI and Alq$_3$ devices. However, the pyridopyrazine derivatives **4** and **6** behave differently. Very weak orange emission was observed for these compounds when TPBI was used as electron transporting layer and this confirms exciton formation inside the HTL layer. However use of Alq$_3$ led to a complex situation with the formation of broad and structureless emission indicative of a recombination zone in both the Alq$_3$ and HTL layers (Table 4). This anomalous behavior could not be explained with certainty at this stage. It is possible that photo-induced electron transfer from **4** and **6** to ETL quench the emission of the molecules.[25] Due to low volatility no device could be fabricated using **8**.

Summary

Quinoxaline/pyridopyrazine–triarylamine conjugates with varied conjugation were prepared by Stille coupling reactions and employed as electroluminescent materials. Experiments varying the device structure for one of the compounds (**3**) unravel the efficient hole transporting property of these materials. Even though a single layer device with reasonable performance

Table 2 Electrochemical data and orbital energies

	Electrochemical data (*vs* ferrocene)		Orbital energies		
Compound	E_{ox} (ΔE_p)/mV	E_{red} (ΔE_p)/mV	HOMO/eV	LUMO/eV	Band gap/eV
3	508 (109)	−2072 (75)	5.31	2.73	2.58
4	521 (109)	−1826 (77)	5.32	2.97	2.35
5	+412 (67), +928 (61)	−1966 (111)	5.21	2.83	2.38
6	+420 (65), +924 (107)	−1809 (71)	5.22	2.99	2.23
7	+354 (78), +752 (75)	−2060 (61)	5.15	2.74	2.41
8	+361 (62), +774 (58)	−1815 (59)	5.16	2.99	2.17

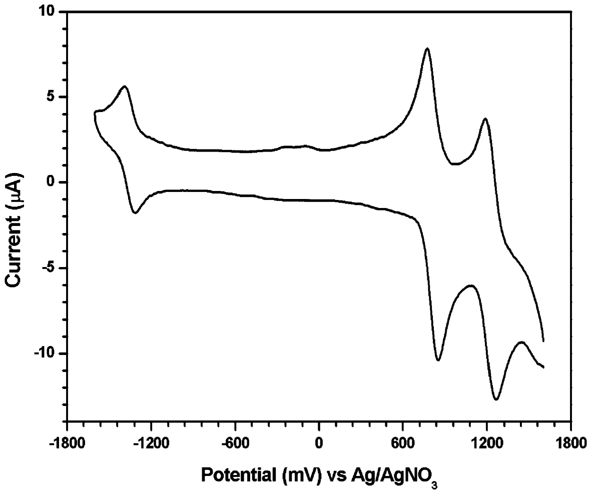

Fig. 2 Cyclic voltammogram of compound **8** measured in dichloromethane solution (scan rate: 100 mV s^{-1}).

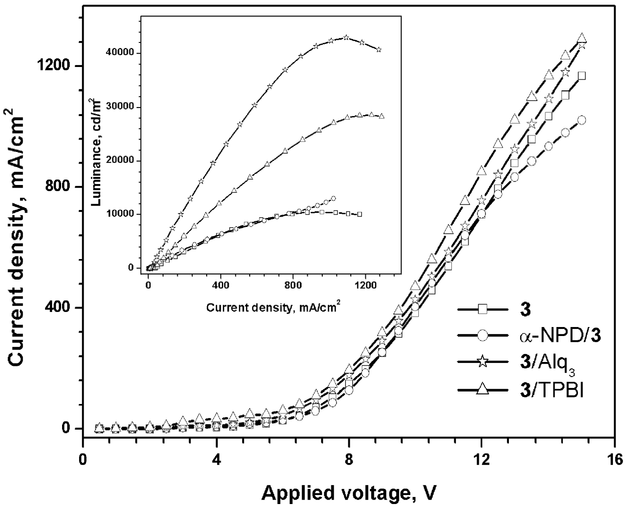

Fig. 3 *I–V–L* curves for the devices fabricated using compound **3**.

Table 3 Electroluminescent characteristics for the compound **3**

Device structure	**3**	NPD/**3**	**3**/TPBI	**3**/Alq_3
Turn-on voltage/V	3.0	2.5	3.2	3.0
Voltage[a]/V	7.4	7.7	6.8	7.1
Brightness[a]/cd m^{-2}	1388	1942	2681	5492
Luminance efficiency[a]/lm W^{-1}	0.6	0.8	1.2	2.4
λ_{em} (FWHM)/nm	548 (82)	544 (72)	542 (92)	544 (102)
λ_{em} (FWHM)/nm (film)	541 (84)			
CIE (x, y)	0.41, 0.57	0.38, 0.59	0.38, 0.57	0.38, 0.56
Maximum brightness/ cd m^{-2} (voltage/V)	10437	13028	28582	42942
Maximum luminance efficiency/lm W^{-1}	0.6	0.8	1.2	2.5

[a] Data taken for the current density 100 mA cm^{-2}.

was fabricated, it was identified that use of an additional electron transfer layer improves the brightness and efficiency significantly.

Experimental

Measurements

Unless otherwise specified, all the reactions were performed under a nitrogen atmosphere using standard Schlenk techniques. Dichloromethane and DMF were distilled from CaH_2 under a nitrogen atmosphere. ^1H spectra were recorded on a Bruker 300 MHz spectrometer operating at 300.135 MHz. Emission spectra were recorded on a PerkinElmer spectrofluorometer, and the quantum efficiencies were obtained by standard method using Coumarin I ($\Phi_f = 0.99$ in ethyl acetate) as reference. All chromatographic separations were carried out on silica gel (60M, 230–400 mesh). Cyclic voltammetry experiments were performed with a BAS-100 electrochemical analyzer. All measurements were carried out at room temperature with a conventional three-electrode configuration consisting of platinum working electrode, an auxiliary platinum electrode, and a non-aqueous Ag/$AgNO_3$ reference electrode. All the experiments were performed with 2.5×10^{-4} M CH_2Cl_2 solutions, and the supporting electrolyte used was 0.1 M tetrabutylammonium hexafluorophosphate. The scan rate was 100 mV s^{-1} and the potential was swept between −2.0 V and +1.5 V. A control experiment was conducted with blank solution at the start to make sure the redox waves observed are due to our materials. The $E_{1/2}$ values were determined as $(E_p^{a} + E_p^{c})/2$, where E_p^{a} and E_p^{c} are the anodic and cathodic peak potentials, respectively. All potentials reported are referenced to a Fc^+/Fc internal standard (+0.350 V relative to the Ag/$AgNO_3$ electrode) and are not corrected for the junction potential. DSC measurements were carried out using a PerkinElmer 7 series thermal analyzer at a heating rate of 10 °C min^{-1}. TGA measurements were performed on a PerkinElmer TGA7 thermal analyzer. Mass spectra (FAB) were recorded on a VG70-250S mass spectrometer. Elementary analyses were performed on a PerkinElmer 2400 CHN analyzer.

General procedure for the C–C coupling (Stille) reactions

The dibromide (**1** or **2**, 1.0 mmol) and the corresponding thienylstannylene (2.2 mmol), $Pd(PPh_3)_2Cl_2$ (140 mg, 0.02 mmol) and dimethyl formamide (20 mL) were mixed together and heated at 70 °C for 12–17 h. After cooling it was quenched with methanol (60 mL). The dark yellow precipitate formed was separated by filtration and purified by column chromatography. The yield generally varied from 60–82% depending on the substrate.

Table 4 Electroluminescent characteristics of compounds **4**, **5**, **6** and **7**

		Compound			
Parameter		**4**	**5**	**6**	**7**
Turn-on voltage/V	TPBI	5.5	2.9	4.0	2.9
	Alq_3	6.0	2.8	4.0	3.0
Voltage[a]/V	TPBI	8.9	6.1	7.8	5.6
	Alq_3	10.6	6.2	8.4	5.2
Brightness[a]/cd m^{-2}	TPBI	60	2696	383	2192
	Alq_3	633	4624	533	868
Luminance efficiency[a]/lm W^{-1}	TPBI	0.02	1.4	0.2	1.2
	Alq_3	0.2	2.3	0.2	0.5
λ_{em} (FWHM)/nm	TPBI	594 (130)	530 (80)	588 (110)	544 (90)
	Alq_3	532 (96)	534 (88)	546 (134)	544 (98)
λ_{em} (FWHM)/nm (film)		592 (131)	527 (81)	594 (112)	538 (96)
CIE (x, y)	TPBI	0.44, 0.47	0.33, 0.59	0.52, 0.46	0.38, 0.56
	Alq_3	0.34, 0.56	0.34, 0.58	0.40, 0.53	0.37, 0.56
Maximum brightness/cd m^{-2}(voltage/V)	TPBI	455	22871	2333	19671
	Alq_3	4144	41167	6853	22366
Maximum luminance efficiency/lm W^{-1}	TPBI	0.02	1.6	0.2	1.3
	Alq_3	0.2	2.4	0.3	0.8

[a] Data taken for the current density 100 mA cm^{-2}.

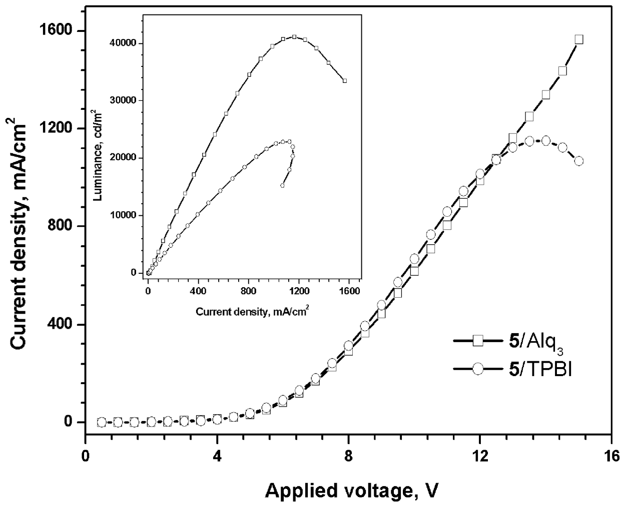

Fig. 4 *I*–*V*–*L* curves of the devices fabricated using compound **5**.

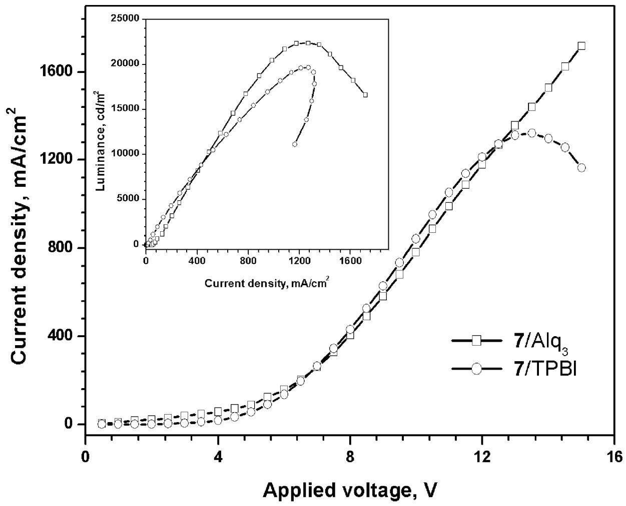

Fig. 5 *I*–*V*–*L* characteristics of the devices fabricated from compound **7**.

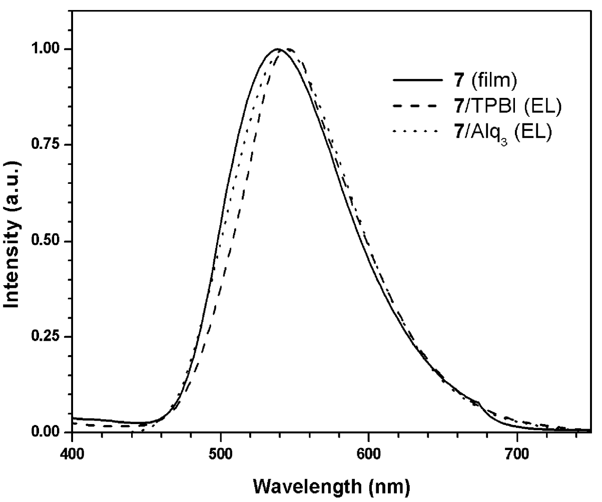

Fig. 6 Film PL and EL spectra of compound **7**.

2,3-Bis-[4-(5-(9-ethylcarbazol-3-yl)thiophen-2-yl)phenyl]quinoxaline (3). Yellow solid. Yield: 78%. ^{1}H NMR (δ, $CDCl_3$): 1.44 (t, 7.3 Hz, 6 H, CH_3), 4.36 (q, 7.3 Hz, 4 H, CH_2), 7.22–7.25 (m, 2 H, carbazole), 7.32 (d, 3.7 Hz, 2 H, thiophene), 7.37–7.49 (m, 8 H), 7.61–7.79 (m, 12 H, carbazole, thiophene, quinoxaline), 8.12 (d, 7.8 Hz, 2 H, carbazole), 8.17–8.21 (m, 2 H, quinoxaline), 8.33 (d, 1. 2 Hz, 2 H, carbazole). FAB MS (*m*/*z*): 833.4 (M^+). Anal. Calcd for $C_{56}H_{40}N_4S_2$: C, 80.74; H, 4.84; N, 6.73. Found: C, 80.65; H, 4.71; N, 6.74%.

2,3-Bis-[4-(5-(9-ethylcarbazol-3-yl)thiophen-2-yl)phenyl]pyrido[2,3-*b*]pyrazine (4). Orange solid. Yield: 66%. ^{1}H NMR (δ, $CDCl_3$): 1.44 (t, 7.3 Hz, 6 H, CH_3), 4.36 (q, CH_2, 4 H), 7.20–7.23 (m, 1 H, pyridine), 7.25–7.50 (m, 10, phenyl, thiophene, carbazole), 7.65–7.78 (m, 12 H, phenyl, carbazole, thiophene), 8.12 (d, 7.3 Hz, 2 H, carbazole), 8.33 (d, 1.2 Hz, 2 H), 8.56 (dd, 8.2, 1.2 Hz, 1 H, pyridine), 9.16–9.18 (m, 1 H, pyridine). FAB MS (*m*/*z*): 833.9 (M^+). Anal. Calcd for $C_{55}H_{39}N_5S_2$: C, 79.20; H, 4.71; N, 8.40. Found: C, 79.01; H, 4.55; N, 8.29%.

2,3-Bis-[4-(5-(4-*N*,*N*-diphenylaminophenyl)thiophen-2-yl)phenyl]quinoxaline (5). Yellow solid. Yield: 82%. ^{1}H NMR (δ, $CDCl_3$): 7.00–7.08 (m, 8 H, ph), 7.10 (d, 8.6 Hz, 8 H, ph), 7.18 (d, 3.7 Hz, 2 H, thiophene), 7.22–7.32 (m, 10 H, ph, thiophene), 7.44–7.49 (m, 4 H, ph), 7.60 (s, 8 H, ph), 7.74–7.79 (m, 2 H, quinoxaline), 8.14–8.18 (m, 2 H, quinoxaline). FAB MS (*m*/*z*): 932 (M^+). Anal. Calcd for $C_{64}H_{44}N_4S_2$: C, 82.37; H, 4.75; N, 6.00. Found: C, 82.31; H, 4.66; N, 5.92%.

2,3-Bis-[4-(5-(4-*N*,*N*-diphenylaminophenyl)thiophen-2-yl)phenyl]pyrido[2,3-*b*]pyrazine (6). Orange solid. Yield: 69%. ^{1}H NMR (δ, CDCl$_3$): 7.00–7.08 (m, 8 H, ph), 7.10 (d, 8.6 Hz, 8 H, ph), 7.19 (d, 3.7 Hz, 2 H, thiophene), 7.23–7.28 (m, 8 H, ph), 7.32 (d, 3. 7 Hz, 2 H, th), 7.46 (d, 8.6 Hz, 4 H, ph), 7.60 (d, 8.6 Hz, 2 H, ph), 7.63 (s, 4 H, ph), 7.67–7.74 (m, 3 H, ph, pyridine), 8.49 (dd, 8.5 Hz, 1 H, pyridine), 9.14 (dd, 8.5, 1.2 Hz, 1 H, pyridine). FAB MS (*m*/*z*): 933 (M$^+$). Anal. Calcd for $C_{63}H_{43}N_5S_2$: C, 81.00; H, 4.64; N, 7.50. Found: C, 81.07; H, 4.55; N, 7.43%.

2,3-Bis-[4-(5-(9,9-diethyl-2-*N*,*N*-diphenylaminofluoren-7-yl)-thiophen-2-yl)phenyl]quinoxaline (7). Yellow solid. Yield: 71%. ^{1}H NMR (δ, CDCl$_3$): 0.38 (t, 7.3 Hz, 12 H, CH$_3$), 1.85–2.017 (m, 8 H, CH$_2$), 6.99–7.12 (m, 15 H), 7.21–7.26 (m, 9 H), 7.34–7.37 (m, 4 H), 7.52–7.67 (m, 16 H), 7.76–7.79 (m, 2 H), 8.17–8.21 (m, 2 H). FAB MS (*m*/*z*): 1220 (M$^+$). Anal. Calcd for $C_{86}H_{68}N_4S_2$: C, 84.55; H, 5.61; N, 4.59. Found: C, 84.51; H, 5.66; N, 4.47%.

2,3-Bis-[4-(5-(9,9-diethyl-2-*N*,*N*-diphenylaminofluoren-7-yl)-thiophen-2-yl)phenyl]pyrido[2,3-*b*]pyrazine (8). Orange solid. Yield: 65%. ^{1}H NMR (δ, CDCl$_3$): 0.38 (t, 7.3 Hz, 12 H, CH$_3$), 1.85–2.03 (m, 8 H, CH$_2$), 6.99–7.11 (m, 17 H), 7.20–7.26 (m, 8 H), 7.34–7.39 (m, 4 H), 7.51–7.77 (m, 18 H), 8.55 (dd, 8.2, 1.2 Hz, 1 H, pyridine), 9.16–9.18 (m, 1 H, pyridine). FAB MS (*m*/*z*): 1221 (M$^+$). Anal. Calcd for $C_{85}H_{67}N_5S_2$: C, 83.50; H, 5.52; N, 5.73. Found: C, 83.36; H, 5.51; N, 5.67%.

Preparation of EL devices and measurements

The electron-transporting materials TPBI and Alq$_3$ were synthesized according to literature procedures[26,27] and were sublimed twice prior to use. Pre-patterned ITO substrates with an effective individual device area of 3.14 mm^2 were cleaned as described in a previous report.[14] Double-layer EL devices using carbazole derivatives as the hole-transport layer and TPBI or Alq$_3$ as the electron-transport layer were fabricated. For comparison, a typical device using 1,4-bis(1-naphthylphenylamino)-biphenyl (α-NPD) as the hole-transport layer was also prepared. All devices were prepared by vacuum deposition of 400 Å of the hole-transport layer, followed by 400 Å of TPBI or Alq$_3$. An alloy of magnesium and silver ($\sim$10 : 1, 500 Å) was deposited as the cathode, which was capped with 1000 Å of silver. The *I*–*V* curve was measured on a Keithley 2400 source meter in an ambient environment. The light intensity was measured with a Newport 1835 optical meter.

Acknowledgements

We are thankful to National Science Council and Academia Sinica for financial support.

References

1 H. Ma and A. K. Y. Jen, *Adv. Mater.*, 2001, **13**, 1201.

2 (*a*) M. Albota, D. Beljonne, J. L. Bredas, J. E. Ehrlich, J. Y. Fu, A. A. Heikal, S. E. Hess, T. Kogej, M. D. Levin, S. R. Marder, D. McCord-Maughon, J. W. Perry, H. Rockel, M. Rumi, C. Subramaniam, W. W. Webb, X. L. Wu and C. Xu, *Science*, 1998, **281**, 1653; (*b*) S. Kawata, H. B. Sun, T. Tanaka and K. Takada, *Nature*, 2001, **412**, 697; (*c*) S. J. Chung, K. S. Kim, T. H. Lin, G. S. He, J. Swiatkiewicz and P. N. Prasad, *J. Phys. Chem. A*, 1999, **103**, 10741; (*d*) R. Kannan, G. S. He, L. X. Yuan, F. M. Xu, P. N. Prasad, A. G. Dombroskie, B. A. Reinhardt, J. W. Baur, R. A. Vaia and L. S. Tan, *Chem. Mater.*, 2001, **13**, 1896.

3 (*a*) X. Q. Lin, B. J. Chen, X. H. Zhang, C. S. Lee, H. L. Kwong and S. T. Lee, *Chem. Mater.*, 2001, **13**, 456; (*b*) C. H. Chen, C. W. Tang, J. Shi and K. P. Klubek, *Thin Solid Films*, 2000, **363**, 327; (*c*) B. J. Jung, C. B. Yoon, H. K. Shim, L. M. Do and T. Zyung, *Adv. Funct. Mater.*, 2001, **11**, 430.

4 (*a*) J. R. Sheats, *Science*, 1997, **277**, 191; (*b*) M. Gross, D. C. Muller, H. G. Nothofer, U. Scherf, D. Neher, C. Brauchle and K. Meerholz, *Nature*, 2000, **405**, 661; (*c*) P. K. H. Ho, D. S. Thomas, R. H. Friend and N. Tessler, *Science*, 1999, **285**, 233; (*d*) Y. Shirota, *J. Mater. Chem.*, 2000, **10**, 1; (*e*) U. Mitschke and P. Bäuerle, *J. Mater. Chem.*, 2000, **10**, 1471.

5 (*a*) N. Tamoto, C. Adachi and K. Nagai, *Chem. Mater.*, 1997, **9**, 1077; (*b*) Z. H. Peng, Z. N. Bao and M. E. Galvin, *Chem. Mater.*, 1998, **10**, 2086; (*c*) W. H. Zhu, H. Tian and A. Elschner, *Chem. Lett.*, 1999, 501.

6 (*a*) Y. Z. Lee, X. W. Chen, S. A. Chen, P. K. Wei and W. S. Fann, *J. Am. Chem. Soc.*, 2001, **123**, 2296; (*b*) E. Diez-Barra, J. C. Garcia-Martinez, S. Merino, R. del Rey, J. Rodriguez-Lopez, P. Sanchez-Verdu and J. Tejeda, *J. Org. Chem.*, 2001, **66**, 5664.

7 (*a*) Y. Z. Wang and A. J. Epstein, *Acc. Chem. Res.*, 1999, **32**, 217; (*b*) Y. X. Yao and J. M. Tour, *Macromolecules*, 1999, **32**, 2455; (*c*) S. C. Ng, H. F. Lu, H. S. O. Chan, A. Fujii, T. Laga and K. Yoshino, *Adv. Mater.*, 2000, **12**, 1122; (*d*) S. C. Ng, H. F. Lu, H. S. O. Chan, A. Fujii, T. Laga and K. Yoshino, *Macromolecules*, 2001, **34**, 6895; (*e*) S. A. Jenekhe, L. D. Lu and M. M. Alam, *Macromolecules*, 2001, **34**, 7315.

8 (*a*) M. Jayakannan, P. A. van Hal and R. A. J. Janssen, *J. Polym. Sci., Part A*, 2002, **40**, 251; (*b*) A. Dhanabalan, J. L. J. van Dongen, J. K. J. van Duren, H. M. Janssen, P. A. van Hal and R. A. J. Janssen, *Macromolecules*, 2001, **34**, 2495.

9 (*a*) M. C. Castex, C. Olivero, G. Pichler, D. Ades, E. Cloutet and A. Siove, *Synth. Met.*, 2001, **122**, 59; (*b*) D. Ades, V. Boucard, E. Cloutet, A. Siove, C. Olivero, M. C. Castex and G. Pichler, *J. Appl. Phys.*, 2000, **87**, 7290.

10 (*a*) S. J. Chung, T. C. Lin, K. S. Kim, G. S. He, J. Swiatkiewicz, P. N. Prasad, G. A. Baker and F. V. Bright, *Chem. Mater.*, 2001, **13**, 4071; (*b*) A. Adronov, J. M. J. Frechet, G. S. He, K. S. Kim, S. J. Chung, J. Swiatkiewicz and P. N. Prasad, *Chem. Mater.*, 2000, **12**, 2838.

11 M. Granstrom, K. Petritsch, A. C. Arias, A. Lux, M. R. Andersson and R. H. Friend, *Nature*, 1998, **395**, 257.

12 K. R. Justin Thomas, J. T. Lin, Y.-T. Tao and C.-W. Ko, *Adv. Mater.*, 2000, **12**, 1949.

13 I.-Y. Wu, J. T. Lin, Y.-T. Tao and E. Balasubramaniam, *Adv. Mater.*, 2000, **12**, 668.

14 K. R. Justin Thomas, J. T. Lin, Y.-T. Tao and C.-W. Ko, *J. Am. Chem. Soc.*, 2001, **123**, 9404.

15 I.-Y. Wu, J. T. Lin, Y.-T. Tao, E. Balasubramaniam, Y.-Z. Su and C.-W. Ko, *Chem. Mater.*, 2001, **13**, 2626.

16 C.-W. Ko, Y.-T. Tao, J. T. Lin and K. R. Justin Thomas, *Chem. Mater.*, 2002, **14**, 357.

17 K. R. Justin Thomas, J. T. Lin, Y.-T. Tao and C.-W. Ko, *Chem. Mater.*, 2002, **14**, 1354.

18 (*a*) T. Yamamoto, K. Sugiyama, T. Kushida, T. Inoue and T. Kanbara, *J. Am. Chem. Soc.*, 1996, **118**, 3930; (*b*) D. O'Brien, M. S. Weaver, D. G. Lidzey and D. D. C. Bradley, *Appl. Phys. Lett.*, 1996, **69**, 881; (*c*) Y. Yang and Q. B. Pei, *Appl. Phys. Lett.*, 1997, **70**, 1926.

19 (*a*) J. F. Wang, Y. Kawabe, S. E. Shaheen, M. M. Morrell, G. E. Jabbour, P. A. Lee, J. Anderson, N. R. Armstrong, B. Kippelen, E. A. Mash and N. Peyghambarian, *Adv. Mater.*, 1998, **10**, 230; (*b*) S. Dailey, W. J. Feast, R. J. Peace, A. C. Sage, S. Till and E. L. Wood, *J. Mater. Chem.*, 2001, **11**, 2238; (*c*) M. Thelakkat, P. Posch and H. W. Schmidt, *Macromolecules*, 2001, **34**, 7441.

20 (*a*) K. R. Justin Thomas, J. T. Lin, Y.-T. Tao and C. H. Chuen, *Chem. Mater.*, 2002, **14**, 2796; (*b*) K. R. Justin Thomas, J. T. Lin, Y.-T. Tao and C. H. Chuen, *Chem. Mater.*, 2002, **14**, 3852.

21 K. R. Justin Thomas, J. T. Lin, Y.-T. Tao and C. H. Chuen, *Adv. Mater.*, 2002, **14**, 822.

22 (*a*) R. E. Gill, A. Hilberer, P. F. van Hutten, G. Berentschot, M. P. L. Werts, A. Meetsma, J. C. Wittmann and G. Hadziioannou, *Synth. Met.*, 1997, **84**, 637; (*b*) J. Daub, R. Engl, J. Kurzawa, S. E. Miller, S. Schneider, A. Stockmann and M. R. Wasielewski, *J. Phys. Chem. A*, 2001, **105**, 5655; (*c*) B. R. Cho, K. H. Son, S. H. Lee, Y. S. Song, Y. K. Lee, S. J. Jeon, J. H. Choi, H. Lee and M. H. Cho, *J. Am. Chem. Soc.*, 2001, **123**, 10039.

23 (*a*) D. F. O'Brien, P. E. Burrows, S. R. Forrest, B. E. Koene, D. E. Loy and M. E. Thompson, *Adv. Mater.*, 1998, **10**, 1108; (*b*) C. Jonda, A. B. R. Mayer, M. Thelakkat, H.-W. Schmidt,

A. Schreiber, D. Haarer and D. Terrell, *Adv. Mater. Opt. Electron.*, 1999, **9**, 117.

24 (*a*) K. Katsumo and Y. Shirota, *Adv. Mater.*, 1998, **10**, 223; (*b*) T. Noda, I. Imae, N. Noma and Y. Shirota, *Adv. Mater.*, 1997, **9**, 239.

25 E. M. Gross, J. D. Anderson, A. F. Slaterbeck, S. Thayumanavan, S. Barlow, Y. Zhang, S. R. Marder, H. K. Hall, M. F. Nabor, J. F. Wang, E. A. Mash, N. R. Armstrong and R. M. Wightman, *J. Am. Chem. Soc.*, 2000, **122**, 4972.

26 (*a*) J. Shi, C. W. Tang and C. H. Chen, *U.S. Pat.*, 5 645 948, 1997; (*b*) A. Y. Sonsale, S. Gopinathan and C. Gopinathan, *Indian J. Chem.*, 1976, **14**, 408.

27 C. H. Chen, J. Shi and C. W. Tang, *Coord. Chem. Rev.*, 1998, **171**, 161.